The Structure of 4-Hydroxybenzoyl-CoA Thioesterase from *Arthrobacter* sp. strain SU*

James B. Thoden‡, Zhihao Zhuang§, Debra Dunaway-Mariano§¶, and Hazel M. Holden‡∥

From the ‡Department of Biochemistry, University of Wisconsin, Madison, Wisconsin 53706-1544 and the §Department of Chemistry, University of New Mexico, Albuquerque, New Mexico 87131

The 4-chlorobenzoyl-CoA dehalogenation pathway in certain *Arthrobacter* and *Pseudomonas* bacterial species contains three enzymes: a ligase, a dehalogenase, and a thioesterase. Here we describe the high resolution x-ray crystallographic structure of the 4-hydroxybenzoyl-CoA thioesterase from *Arthrobacter* sp. strain SU. The tetrameric enzyme is a dimer of dimers with each subunit adopting the so-called "hot dog fold" composed of six strands of anti-parallel β-sheet flanked on one side by a rather long α-helix. The dimers come together to form the tetramer with their α-helices facing outwards. This quaternary structure is in sharp contrast to that previously observed for the 4-hydroxybenzoyl-CoA thioesterase from *Pseudomonas* species strain CBS-3, whereby the dimers forming the tetramer pack with their α-helices projecting toward the interfacial region. In the *Arthrobacter* thioesterase, each of the four active sites is formed by three of the subunits of the tetramer. On the basis of both structural and kinetic data, it appears that Glu[73] is the active site base in the *Arthrobacter* thioesterase. Remarkably, this residue is located on the opposite side of the substrate-binding pocket compared with that observed for the *Pseudomonas* enzyme. Although these two bacterial thioesterases demonstrate equivalent catalytic efficiencies, substrate specificities, and metabolic functions, their quaternary structures, CoA-binding sites, and catalytic platforms are decidedly different.

During the last century, large quantities of 4-chlorobenzoate or related herbicides and polychlorinated biphenyl pesticides were released into the environment because of commercial production and careless waste disposal (1–4). Strikingly, a variety of soil-dwelling bacteria capable of employing 4-chlorobenzoate as their principal source of carbon have been discovered in richly contaminated areas (5–7). In these microorganisms, 4-chlorobenzoate is first converted to 4-hydroxybenzoate, which is subsequently metabolized via the *ortho-* or *meta-*cleavage pathways (5). The 4-chlorobenzoate dehalogenation pathway, as outlined in Scheme 1, consists of three reaction steps catalyzed by 4-chlorobenzoyl-CoA ligase, 4-chlorobenzoyl-CoA dehalogenase, and 4-hydroxybenzoyl-CoA thioesterase (8). Genes encoding these enzymes are organized within an operon that is under the regulatory control of 4-chlorobenzoate (5). In some bacteria, the gene cluster is located within the chromosomal DNA (12–14), whereas in others it is plasmid-encoded (15, 16).

The 4-chlorobenzoyl-CoA pathway operons of certain *Arthrobacter* and *Pseudomonas* bacterial strains display significant differences in both gene order and sequences (17). At the primary structural level, the amino acid sequence identity between paired *Arthrobacter* and *Pseudomonas* ligases is ~38%, whereas that between paired dehalogenases is ~50%. Remarkably, however, there is no significant amino acid sequence identity shared between the thioesterases from these species.

The three-dimensional structure of the thioesterase from *Pseudomonas* sp. strain CBS-3 was solved several years ago in this laboratory and was shown to have a "hot dog fold" motif (18, 19). This type of molecular architecture was first observed in the x-ray structure of β-hydroxydecanoyl thiol ester dehydrase from *Escherichia coli* (20) and has since been found in the (*R*)-specific enoyl-CoA hydratase from *Aeromonas caviae* (21). The structures of these enzymes are dominated by a five-stranded anti-parallel β-sheet that cradles a rather long α-helix of approximately five turns.

Here we report a high resolution x-ray crystallographic analysis of the *Arthrobacter* sp. strain SU 4-hydroxybenzoyl-CoA thioesterase complexed with its products (4-hydroxybenzoate and CoA) or with the substrate analogs, 4-hydroxyphenacyl-CoA or 4-hydroxybenzyl-CoA (Scheme 2). Although the overall topology of the *Arthrobacter* thioesterase subunit is similar to that described for the *Pseudomonas* enzyme, its quaternary structure, CoA-binding site, and catalytic platform are different.

EXPERIMENTAL PROCEDURES

Enzyme Purification and Crystallization—Recombinant *Arthrobacter* sp. strain SU 4-hydroxybenzoyl-CoA thioesterase ($k_{cat} = 6.7$ s^{-1} and $K_m = 1.2$ μM at pH 7.5 and 25 °C; k_{cat} optimal over pH range of 6–10) was purified as previously described (17). 4-Hydroxyphenacyl-CoA or 4-hydroxybenzyl-CoA was prepared according to published procedures (19, 22).
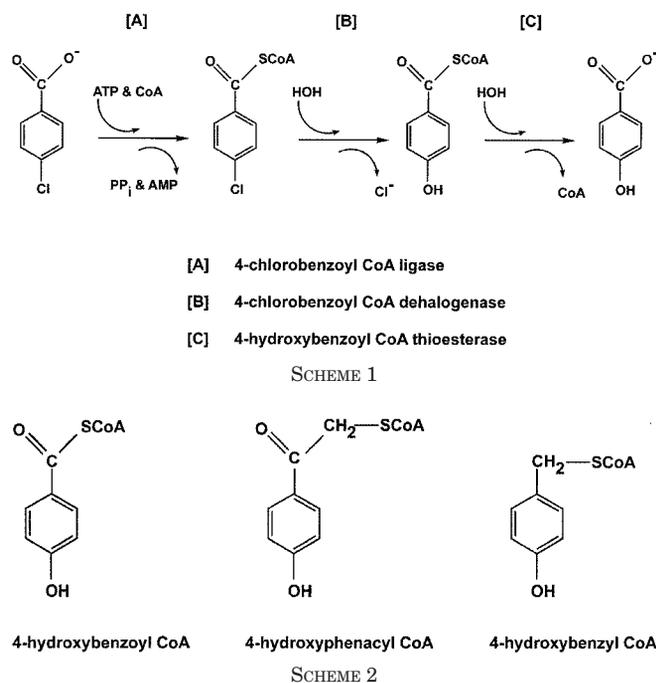
A search for crystallization conditions was conducted utilizing a sparse matrix screen (designed "in-house") composed of 144 conditions at both room temperature and at 4 °C via the hanging drop method of vapor diffusion. The conditions were tested with both the apo enzyme and that complexed with 1 mM 4-hydroxyphenacyl-CoA. The protein solution, at a concentration of 18 mg/ml, contained 10 mM HEPES (pH 7.5), 150 mM KCl, and 1 mM 1,4-dithio-D,L-threitol. The best crystals were observed growing at room temperature from poly(ethylene glycol) 3400 at pH 7.0 in the presence of 4-hydroxyphenacyl-CoA. Large single crystals were subsequently obtained via hanging drops with precipitant

¶ To whom correspondence may be addressed: Dept. of Chemistry, University of New Mexico, Albuquerque, NM 87131. Tel.: 505-277-3383; Fax: 505-277-6202; E-mail: dd39@unm.edu.

∥ To whom correspondence may be addressed: Dept. of Biochemistry, 433 Babcock Dr., University of Wisconsin, Madison, WI 53706-1544. Tel.: 608-262-4988; Fax: 608-262-1319; E-mail: Hazel_Holden@biochem.wisc.edu.

[A] 4-chlorobenzoyl CoA ligase

[B] 4-chlorobenzoyl CoA dehalogenase

[C] 4-hydroxybenzoyl CoA thioesterase

SCHEME 1

4-hydroxybenzoyl CoA   4-hydroxyphenacyl CoA   4-hydroxybenzyl CoA

SCHEME 2

solutions containing 17–20% poly(ethylene glycol) 3400, 100 mM MOPS[1] (pH 7.0), and 200 mM LiCl. The crystals achieved maximum dimensions of 0.7 mm × 0.7 mm × 0.3 mm in ~1–2 weeks. They belonged to the trigonal space group P3$_2$21 with unit cell dimensions of $a = b = 113.2$ Å and $c = 62.5$ Å and contained one dimer in the asymmetric unit. The crystals of the enzyme complexed with either 4-hydroxybenzoyl-CoA or 4-hydroxybenzyl-CoA were prepared in a similar manner. It was never possible to grow crystals of the apo enzyme in a form suitable for a high resolution x-ray analysis.

Structural Analysis of the Thioesterase/4-Hydroxyphenacyl-CoA Complex—An initial x-ray data set was collected to 2.6 Å resolution at 4 °C with a Bruker HISTAR area detector system equipped with Supper long mirrors. The x-ray source was CuKα radiation from a Rigaku RU200 x-ray generator operated at 50 kV and 90 mA. The x-ray data were processed with XDS (23, 24) and internally scaled with XSCALI-BRE.[2] The x-ray data collection statistics are presented in Table I.

One isomorphous heavy atom derivative was prepared by soaking a crystal in 1 mM methylmercury acetate for 1 day. The x-ray data (including Friedel mates) were collected to 2.6 Å. The *R*-factor between the native and mercury derivative x-ray data sets was 26.8% (where $R = \Sigma|F_N - F_h|/\Sigma|F_N| \times 100$, F_N is the native structure factor amplitude and F_h is the heavy-atom derivative structure factor amplitude). Four heavy atom-binding sites were determined with CNS (25). The positions, occupancies, and temperature factors for these sites were refined with CNS, yielding an overall figure of merit of 0.44 and a phasing power of 1.58. Protein phases were calculated to 2.6 Å resolution with CNS and improved by the method of solvent flipping (as implemented in CNS) to yield a figure of merit of 0.94. Greater than 95% of the residues were built into the solvent flattened electron density map with the graphics software TURBO (26). This "partial" model was subsequently refined via least squares with the program package TNT (27). The resulting electron density maps calculated with coefficients of the form $(2F_o - F_c)$ or $(F_o - F_c)$ allowed for the placement of the remainder of the amino acid residues and the 4-hydroxyphenacyl-CoA ligand.

High Resolution X-ray Data Collection and Least Squares Refinement—Thioesterase crystals were harvested from hanging drop experiments and equilibrated in a synthetic mother liquor composed of 20% poly(ethylene glycol) 3400, 150 mM KCl, 100 mM LiCl, 1 mM 4-hydroxyphenacyl-CoA, and 100 mM MOPS (pH 7.0). They were then serially transferred to a cryoprotectant solution containing 30% poly(ethylene glycol) 3400, 200 mM KCl, 250 mM LiCl, 15% ethylene glycol, 1 mM 4-hydroxyphenacyl-CoA, and 100 mM MOPS (pH 7.0). The crystals were suspended in a loop of 20-μm nylon and flash frozen in a stream of

nitrogen gas. Unit cell dimensions changed to $a = b = 112.5$ Å and $c = 60.6$ Å upon cooling to 120 K. A native x-ray data set was collected to 1.6 Å resolution, processed with SAINT (Bruker AXS, Inc.), and scaled as previously described. This structure was solved via molecular replacement with the program AMORE (28) employing as the search model the refined structure determined at 2.6 Å resolution. Iterative cycles of least squares refinement and manual model building reduced the *R*-factor to 18.0% for all measured x-ray data from 30.0 to 1.6 Å resolution. The least squares refinement statistics are presented in Table II.

Structure Determination of the Thioesterase Complexed with 4-Hydroxybenzoyl-CoA (Substrate) or 4-Hydroxybenzyl-CoA—These two structures were solved by difference Fourier techniques with the initial models lacking ordered solvent molecules and ligands. The complex of the enzyme with bound products was prepared by crystallizing the enzyme in the presence of its substrate, 4-hydroxybenzoyl-CoA that was hydrolyzed to 4-hydroxybenzoate (or 4-hydroxybenzoic acid) and CoA. For the sake of simplicity, the ligand will be referred to as 4-hydroxybenzoate, but this does not imply that its protonation state is known. All of the x-ray data for these two complexes were collected in a manner identical to that employed for the thioesterase/4-hydroxyphenacyl-CoA complex as described above. Relevant x-ray data collection and least squares refinement statistics are given in Tables I and II, respectively. In all three complexes, the first 10 and 11 residues were disordered in subunits I and II, respectively. Apart from these disordered N-terminal residues, the electron densities corresponding to both polypeptide chains in the asymmetric unit were continuous throughout the map. The only significant outlier in the Ramachandran plot was Asp[39] (in both subunits). This residue is located ~14 Å from the active site. The dihedral angles adopted by Asp[39] produce a bulge in the first β-strand of the sheet. All of the figures were prepared with the software package MOLSCRIPT (29).

Ligand Binding—The initial velocity of the thioesterase catalyzed hydrolysis of 4-hydroxybenzoyl-CoA was measured by monitoring the decrease in solution absorption at 300 nm resulting from the disappearance of reactant ($\Delta\epsilon = 11.8$ mM^{-1}·cm^{-1}). The reactions were carried out in 50 mM K$^+$-HEPES (pH 7.5, 25 °C) that contained 0.003 μM thioesterase, varying concentrations of 4-hydroxybenzoyl-CoA (1–10 μM) and varying concentrations of 4-hydroxyphenacyl-CoA (0.00925, 0.00185, and 0.037 μM) or 4-hydroxybenzyl-CoA (0.38, 0.76, 1.9, and 3.8 μM). The initial velocity data were analyzed using Equation 1 and the computer program KinetAsyst (IntelliKinetics, PA).

$$V = V_{max}[S]/[K_m(1 + [I]/K_i) + [S]] \qquad \text{(Eq. 1)}$$

where V = initial velocity, V_{max} = maximum velocity, [S] = substrate concentration, K_m = Michaelis constant, [I] = inhibitor concentration, and K_i = the inhibition constant.

RESULTS AND DISCUSSION

Inhibitor Binding—The binding constants of the substrate analogs were evaluated by measuring their competitive inhibition constants. Both analogs displayed linear competitive inhibition *versus* 4-hydroxybenzoyl-CoA. The K_i of 4-hydroxybenzyl-CoA was 0.6 ± 0.1 μM, and the K_i of 4-hydroxyphenacyl-CoA was 0.003 ± 0.0003 μM. These results indicate that these ligands bind tightly to the substrate-binding site.

Overall Structure of the Thioesterase/Product Complex—All of the crystals employed in this investigation contained two subunits/asymmetric unit. For the sake of simplicity, the following discussions will refer only to Subunit II of the x-ray coordinate file unless otherwise indicated. A ribbon representation of the monomer with the bound products, 4-hydroxybenzoate and CoA, is depicted in Fig. 1. The monomer contains 151 amino acid residues, and its topology, referred to as the hot dog fold, is dominated by a six-stranded anti-parallel β-sheet formed by Val[37]–Met[41], Ala[46]–Val[52], Met[89]–Phe[100], His[108]–Ala[118], Trp[123]–Arg[130], and Arg[135]–Arg[149]. These β-strands are labeled *A–F* in Fig. 1. Four of the six β-strands (*A, C, D,* and *F*) contain β-bulges at Asp[39] ($\phi = -101°$, $\psi = -73°$), Gln[94] ($\phi = -115°$, $\psi = -30°$), Ile[116] ($\phi = -113°$, $\psi = -20°$), and Cys[137] ($\phi = -94°$, $\psi = -29°$), respectively. In addition to the six β-strands, there are two α-helices delineated by Leu[30]–Val[34] and Gly[65]–Val[84], six Type I turns, and one Type III turn.

[1] The abbreviation used is: MOPS, 3-(*N*-morpholino)propanesulfonic acid.

[2] I. Rayment and G. Wesenberg, unpublished results.

TABLE I
X-ray data collection statistics

Data Set	Resolution	Independent reflections	Completeness	Redundancy	Avg *I*/Avg $\sigma(I)$	$R_{sym}{}^a$
	Å		%			
Enzyme/(4-hydroxyphenacyl-CoA complex)	30.0-2.60	14,133	97.6	6.8	6.3	8.0
	2.72-2.60^b	1448	79.5	2.3	1.5	25.4
Mercury derivative	30.0-2.60	14,405	98.6	5.7	9.8	7.5
	2.72-2.60	1737	94.8	2.9	1.9	24.4
Enzyme/(4-hydroxyphenacyl-CoA complex)	30.0-1.60	58,417	97.1	7.4	35.1	4.9
	1.66-1.60	4693	81.0	3.7	1.7	39.1
Enzyme/(4-hydroxybenzyl-CoA complex)	30.0-1.60	57,216	97.6	7.2	39.1	4.1
	1.66-1.60	5007	86.3	3.2	2.1	29.6
Enzyme/(4-hydroxybenzoyl-CoA)	30.0-1.95	30,625	94.1	3.6	24.6	5.1
	2.04-1.95	3403	83.4	1.9	4.1	22.0

^{a} $R_{sym} = (\Sigma \ |I - \bar{I}|/\Sigma \ I) \times 100$.
^{b} Statistics for the highest resolution bin.

TABLE II
Least squares refinement statistics

Complex	4-Hydroxyphenacyl-CoA	4-Hydroxybenzyl-CoA	Products
Resolution limits (Å)	30.0-1.60	30.0-1.60	30.0-1.95
R-factor (overall) (%/no. rflns)^a	18.0/58147	17.5/57011	18.3/30567
R-factor (working) (%/no. rflns)	17.9/52320	17.3/51034	18.2/27534
R-factor (free) (%/no. rflns)	21.9/5827	21.3/5707	23.7/3303
No. protein atoms	2180^b	2153^c	2163^d
No. hetero-atoms	428^e	425^f	357^g
Bond lengths (Å)	0.012	0.012	0.013
Bond angles (deg)	2.25	2.36	2.24
Trigonal planes (Å)	0.007	0.006	0.007
General planes (Å)	0.012	0.013	0.012
Torsional angles (deg)^h	16.9	17.2	17.2

^{a} R-factor = $(\Sigma|F_o - F_c|/\Sigma|F_o|) \times 100$ where F_o is the observed structure-factor amplitude and F_c is the calculated structure-factor amplitude.
^{b} These include multiple conformations for Glu^{27}, Asp^{39}, Val^{114}, Ser^{128}, and Ser^{140} in Subunit I and Glu^{27}, Asp^{39}, Ser^{128}, and Ser^{140} in Subunit II.
^{c} These include multiple conformations for Leu^{30}, Gln^{94}, Lys^{105}, and Ser^{128} in Subunit I and Glu^{27}, Glu^{94}, and Ser^{140} in Subunit II.
^{d} These include multiple conformations for Asp^{17} in Subunit I and Asp^{39}, Gln^{94}, and Ser^{120} in Subunit II.
^{e} These include two 4-hydroxyphenacyl-CoA moieties, four chloride ions, three ethylene glycols, and 296 waters.
^{f} These include two 4-hydroxybenzyl-CoA moieties, one ethylene glycol, and 301 waters.
^{g} These include two CoA molecules, two 4-hydroxybenzoate moieties, and 241 waters.
^{h} The torsional angles were not restrained during the refinement.
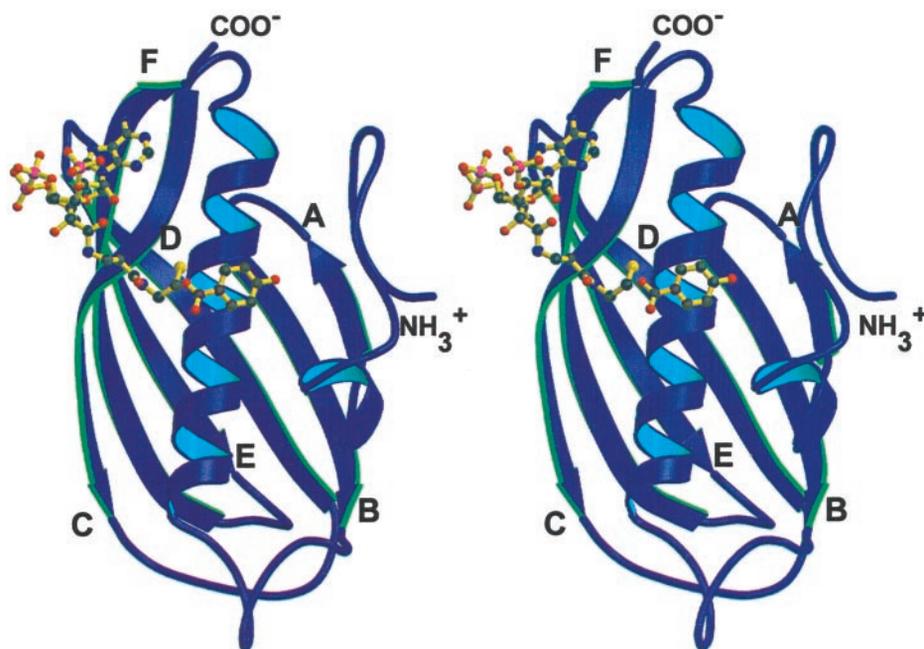
FIG. 1. **Ribbon representation of the *Arthrobacter* thioesterase monomer.** The bound ligands, 4-hydroxybenzoate and CoA, are shown in ball-and-stick representations.

Nearly 80% of the amino acid residues lie within classical secondary structural elements. The monomer is compact with overall dimensions of ~38 Å × 49 Å × 35 Å.

In that the asymmetric unit contained only two subunits, ultracentrifugation experiments were subsequently performed to define the quaternary structure of the *Arthrobacter* thioesterase. These experiments were consistent with a tetrameric quaternary structure. The tetramer thus packed in the crystalline lattice with one of its 2-fold rotational axes coincident to a crystallographic dyad. Shown in Fig. 2*a* is a ribbon represen-
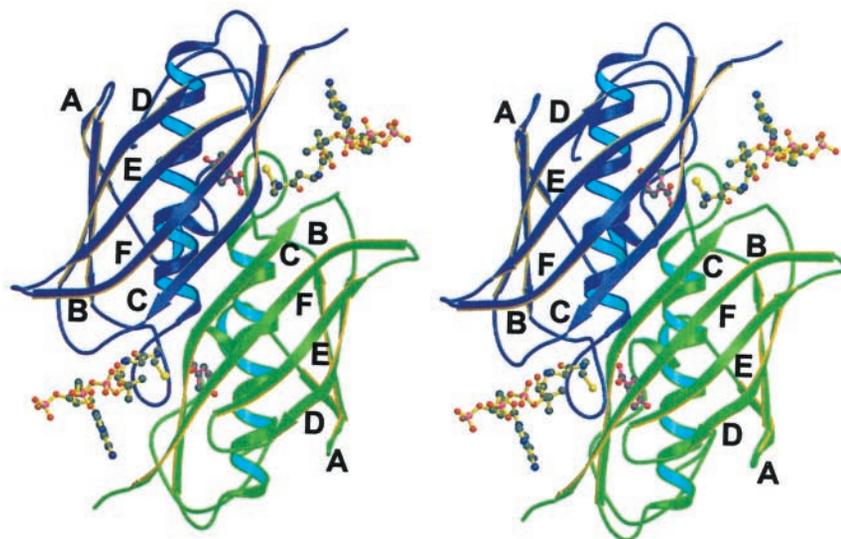
(a)

FIG. 2. **Quaternary structure of the *Arthrobacter* thioesterase.** The quaternary structure of the enzyme can be aptly described as a dimer of dimer. The dimer is shown in *panel a* with the two separate subunits displayed in *blue* and *green*. The 4-hydroxybenzoate and CoA moieties are drawn in ball-and-stick representations with *pink*- and *yellow*-filled bonds, respectively. The complete tetramer is depicted in *panel b* with the long α-helices, one per subunit, displayed as cylinders. Key amino acid residues involved in dimer-dimer interactions are shown in ball-and-stick representations with *green*-filled bonds. For comparison purposes, the *Pseudomonas* thioesterase tetramer, complexed with 4-hydroxybenzyl-CoA, is presented in *panel c*.
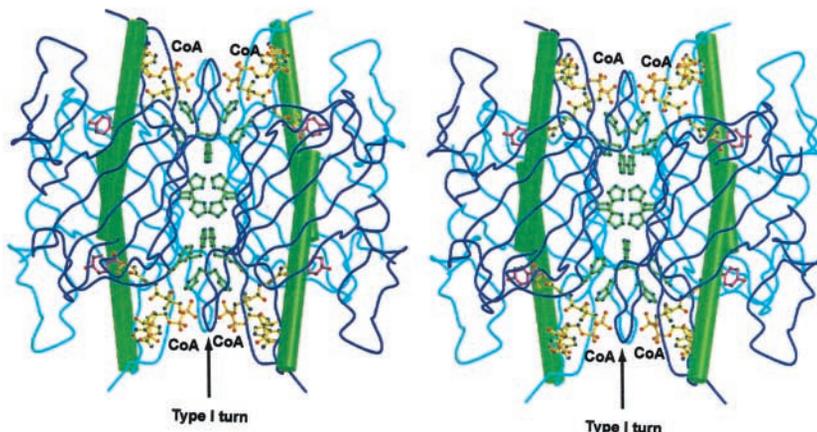
(b)
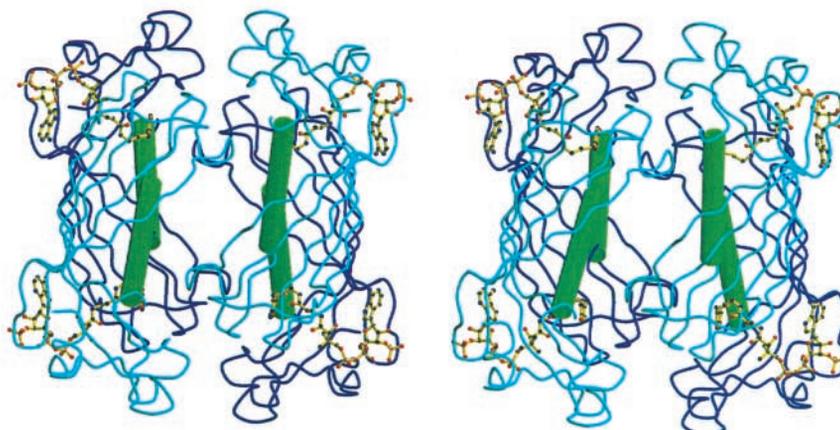
(c)

FIG. 3. **The *Arthrobacter* thioesterase active site with bound hydrolysis products.** Those residues located within ~3.5 Å of the 4-hydroxybenzoate and CoA molecule are shown. The products are highlighted in *yellow*-filled bonds. Ordered water molecules are represented by the *red spheres*. The *asterisks* indicate those amino acid residues belonging to Subunit II. Ser[120] and Thr[121], highlighted in *pink*-filled bonds, belong to Subunit III of the tetramer.
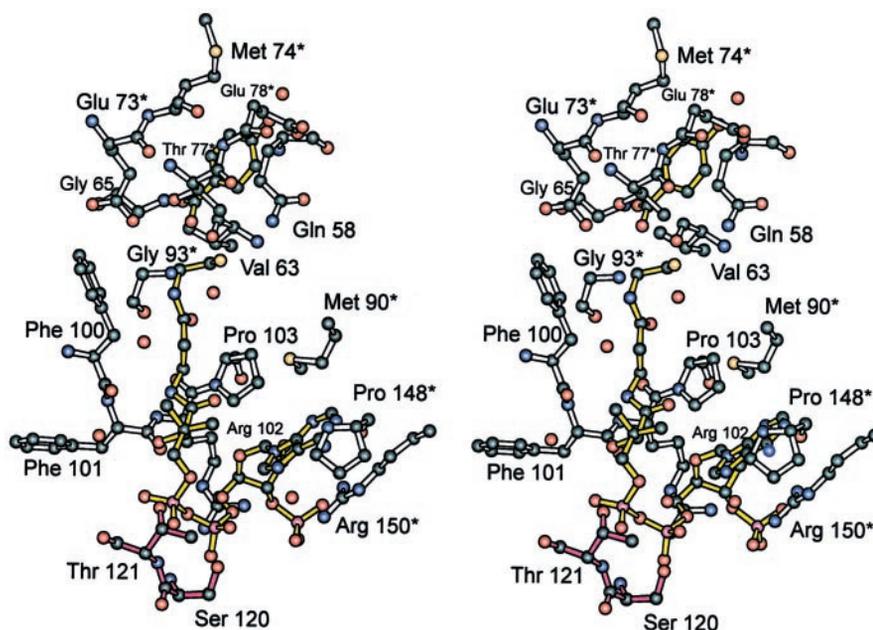
tation of the two monomers contained within the asymmetric unit. The tetrameric form of the enzyme, as depicted in Fig. 2*b*, was generated by rotation of the dimer in the asymmetric unit about the crystallographic 2-fold rotational axis. As can be seen from Fig. 2 (*a* and *b*), the quaternary structure of the enzyme can be aptly described as a dimer of dimers with overall dimensions of ~72 Å × 70 Å × 52 Å.

The subunit-subunit interface of the dimer is quite extensive with a total buried surface area of ~3100 Å^2 as calculated according to the method of Lee and Richards (30). There are three major regions of subunit-subunit interactions between the two monomers. These intermolecular contacts are formed by Tyr[22]–Val[34] (α-helix), Asp[54]–Met[74] (α-helix), and Gly[93]–Pro[103] (β-strand C) in one subunit and the symmetry-related residues in the second monomer. Indeed, the six-stranded sheets in each monomer come together, through β-strands C, to form a 12-stranded anti-parallel β-sheet in the dimer. The active sites are wedged between the two subunits of the dimer and are separated by ~24 Å (Fig. 2*a*). The two major α-helices of the dimer run anti-parallel to one another.

The 12-stranded β-sheet of one dimer abuts the β-sheet motif in the second dimer to form the tetramer (Fig. 2*b*). This packing arrangement is reminiscent to that observed for the dimeric thioesterase II from *E. coli* (31). In this enzyme, each monomer contains two hot dog folds referred to as the "double hot dog." The subunit-subunit interface for the *E. coli* thioesterase II is likewise built with the β-sheets back to back and the major α-helices facing outwards.

Approximately 2125 Å^2 of surface area is buried per monomer upon tetramer formation in the *Arthrobacter* thioesterase. The dimer-dimer interface is lined with water molecules and various side chains from each subunit including His[97], Phe[101], His[117], and Phe[124]. As can be seen in Fig. 2*b*, the histidines at position 97 form a hydrogen bonding ring at the middle of the dimer-dimer interface. The pyrophosphate groups of the CoA moieties project into this interface. Ser[120] and Thr[121], which lie in a Type I turn defined by Gly[119]–Thr[122], provide hydrogen bonds to the phosphoryl oxygens of the CoA. Specifically, O$^\gamma$ and the peptidic NH group of Ser[120] lie within hydrogen bonding distance to the two α-phosphoryl oxygens, respectively, whereas O$^\gamma$ and the peptidic NH group of Thr[121] are situated within ~2.5 Å of one of the β-phosphoryl oxygens. Each of the
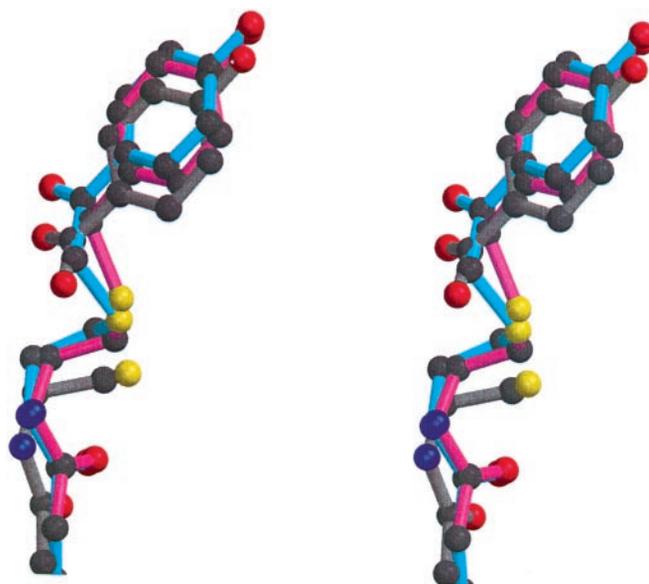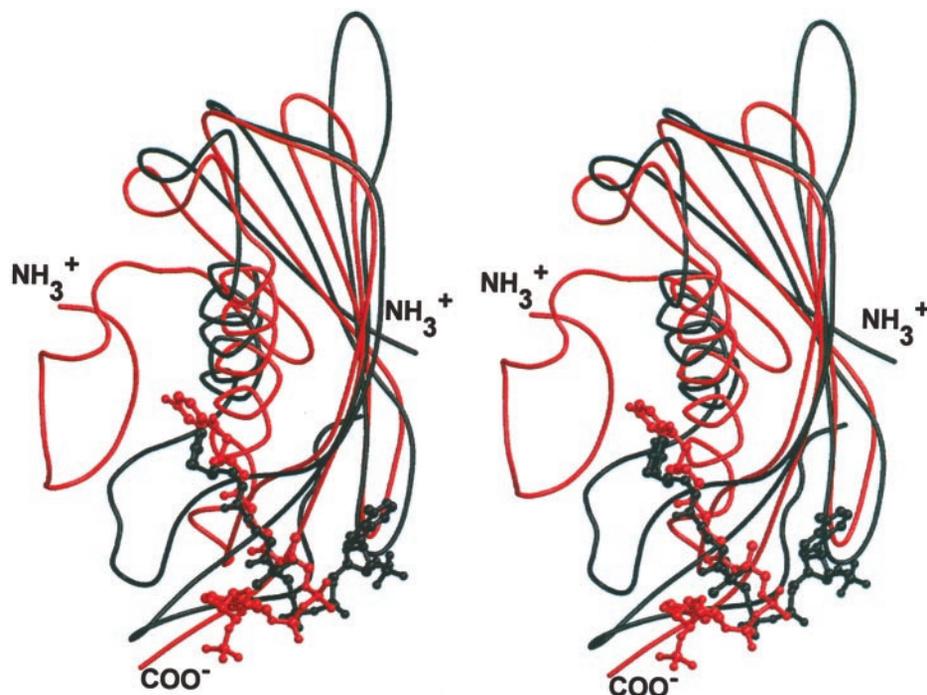

FIG. 4. **Inhibitor binding to the *Arthrobacter* thioesterase.** A superposition of the two inhibitors, 4-hydroxybenzyl-CoA (*pink*) and 4-hydroxyphenacyl-CoA (*blue*) onto the bound hydrolysis products, 4-hydroxybenzoate and CoA (*gray*).

binding sites for CoA is thus formed by three of the four subunits comprising the tetramer.

Active Site with Bound Products, 4-Hydroxybenzoate and CoA—As can be seen from Fig. 2*a*, the 4-hydroxybenzoate is primarily wedged between the two subunits of the dimer pair in the tetramer and specifically between the two major α-helices. A close-up view of the active site is presented in Fig. 3. Key side chains involved in binding the 4-hydroxybenzoate moiety to the protein include Glu[73], Thr[77], and Glu[78] from Subunit II. In addition, the 4-hydroxyl group lies within hydrogen bonding distance to an ordered water molecule, whereas one of the carboxylate oxygens hydrogen bonds to the peptidic NH group of Gly[65] in Subunit I. One of the carboxylate oxygens of the 4-hydroxybenzoate ligand is positioned within 2.8 Å of the sulfhydryl group of CoA, indicating that the substrate has indeed been hydrolyzed. The CoA binds to the protein in a quite curved conformation with its ribose adopting the C$_{3'}$-*endo* con-

formation. Only solvent molecules and backbone carbonyl or peptidic NH groups lie within hydrogen bonding distance to the oxygens and nitrogens of the CoA β-mercaptoethylamine and pantothenate units. The pyrophosphate group oxygens of CoA, however, form hydrogen bonds with the side chains of Ser[120] and Thr[121] situated in the third subunit of the tetramer. Two arginine residues, 102 from Subunit I and 150 from Subunit II, point toward the 3′-phosphate group of the CoA ribose. Additionally, the side chain of Arg[150] (Subunit II) runs nearly parallel to the plane of the adenine ring. The amino group at position 6 of the adenine ring forms hydrogen bonds with a water molecule and the carbonyl oxygen of Pro[148] from Subunit II.

Structure of the Arthrobacter Thioesterase Complexed with Either 4-Hydroxyphenacyl-CoA or 4-Hydroxybenzyl-CoA—The binding of either 4-hydroxyphenacyl-CoA or 4-hydroxybenzyl-CoA within the thioesterase active site resulted in little perturbation of the polypeptide chain backbone compared with that were observed with bound products. Indeed, the α-carbons for these two complexes both superimpose onto the protein/product complex with a root mean square deviation of 0.17 Å. For all atoms, the three models presented here superimpose upon one another with typical root mean square deviations of 0.45 Å or less. In all three of the complexes, the conformations of the side chains lining the active sites are identical within experimental error. A superposition of the three ligands bound to the protein is presented in Fig. 4.

The K_i of 4-hydroxybenzyl-CoA is 0.6 ± 0.1 μM. As can be seen in Scheme 2, the carbonyl functional group of the substrate has been replaced by a methylene bridge in 4-hydroxybenzyl-CoA. The electron density for this inhibitor is indicative of two conformations with the sulfur atoms of the CoA differing by ~1.8 Å. Interestingly, the K_i of 4-hydroxyphenacyl-CoA is considerably lower at 0.003 ± 0.0003 μM. In this inhibitor, an additional methylene group has been inserted between the 4-hydroxybenzoyl and the CoA moieties (Scheme 2). It is possible that this inhibitor is a mimic for the transition state as the carbon-sulfur bond lengthens during substrate hydrolysis.

Structure Comparison of the Arthrobacter Enzyme with the Thioesterase Isolated from Pseudomonas sp. Strain CBS3—The first thioesterase structure to be solved in the 4-chlorobenzoyl-

CoA degrading pathway was that isolated from *Pseudomonas* sp. strain CBS3 (18, 19). Each subunit of this enzyme is characterized by a five-stranded anti-parallel β-sheet and three major α-helices. The *Arthrobacter* thioesterase monomer, with 151 amino acids, is slightly larger than the *Pseudomonas* enzyme (141 amino acids). A superposition of these enzymes, both complexed with 4-hydroxyphenacyl-CoA, is given in Fig. 5. In the *Arthrobacter* enzyme, residues Gly[12]–Pro[43] fold into a short α-helix and the first β-strand of the β-sheet. There are no structural counterparts in the *Pseudomonas* protein. Indeed, the two enzymes start to superimpose at Glu[44] and Arg[3] for the *Arthrobacter* and *Pseudomonas* enzymes, respectively. Those regions of structural correspondence between these two thioesterases superimpose with a root mean square deviation of 1.4 Å for 73 equivalent α-carbons.

In both thioesterases, the two subunits orient in an antiparallel fashion to form the dimers (Fig. 2). In the case of the *Arthrobacter* thioesterase, the third β-strands in each monomer lie at the dimeric interface and form backbone hydrogen bonds via Gln[94], Asn[96], Thr[98], and Phe[100] in each subunit. In the *Pseudomonas* thioesterase, the second β-strands of the monomers interact at the dimeric interface through hydrogen bonds formed by the backbone atoms of Val[62], Cys[64], Ala[66], and Phe[68] in each subunit.

From Figs. 2 and 5, it can be seen that the 4-hydroxyphenacyl ligands bind to the two thioesterases in distinctively different manners. In the *Pseudomonas* thioesterase, the 4′-phosphopantetheine portion of the CoA winds to the right as it reaches the solvent, thereby allowing a phosphoryl oxygen to interact with the backbone nitrogen of Ala[129] in its extra C-terminal appendage and the 3′-phosphate group to hydrogen bond with the backbone peptidic NH groups positioned in the reverse turn connecting the third and fourth β-strands. In the *Arthrobacter* thioesterase, the 4′-phosphopantetheine moiety winds to the left as it reaches the solvent, thereby positioning the nucleotide to interact with Arg[102] in Subunit I and Pro[148] and Arg[150] in Subunit II. The nucleotide is thus directed toward the center of the dimer-dimer interface where it interacts with residues contributed by a third monomer in the tetramer (Fig. 2b). Despite the common hot dog scaffold in these thioes-
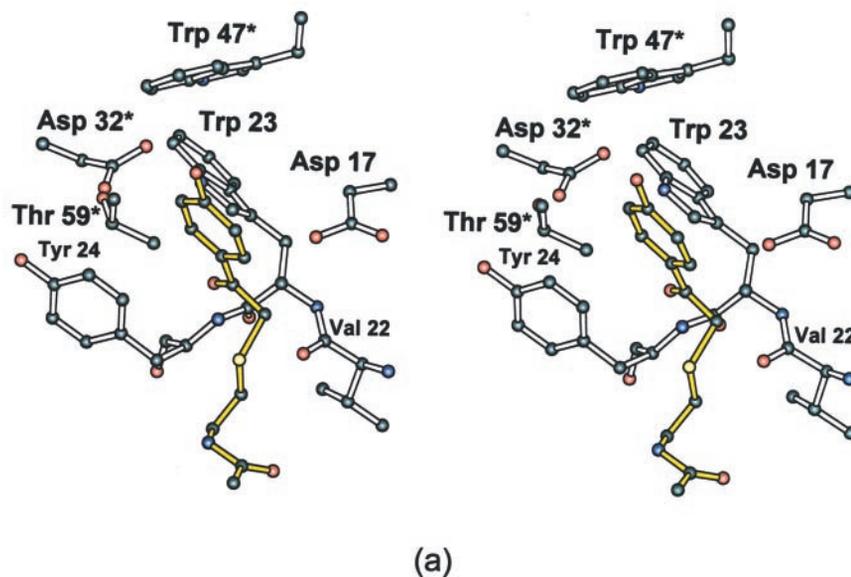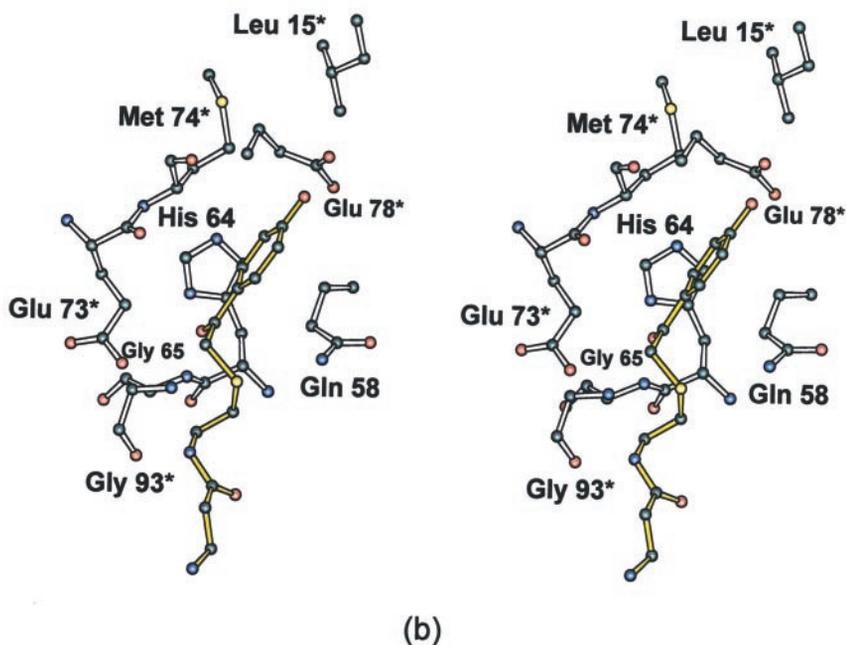
(a)

FIG. 6. **The active sites for the *Pseudomonas* and *Arthrobacter* thioesterases with 4-hydroxyphenacyl-CoA.** The active sites for the *Pseudomonas* and *Arthrobacter* enzymes are shown in *panels a* and *b*, respectively. Residues marked by *asterisks* belong to the second subunit of the dimer.

(b)

terases, the substrate-binding sites are not similar, and the differences are apparently a function of the differing N- and C-terminal regions.

In both thioesterases, the 4-hydroxyphenacyl moieties are positioned into the core of the protein such that the thioester C=O interacts with the N terminus of the major α-helix via a hydrogen bond to the backbone amide NH (Tyr[24] in the *Pseudomonas* thioesterase and Gly[65] in the *Arthrobacter* enzyme). This interaction, which leads to polarization of the C=O for nucleophilic attack (18, 19) is thought to be an important component of the catalytic mechanism. The other essential component is believed to be an active site carboxylate residue that mediates the hydrolysis reaction via either nucleophilic or general base catalysis. In the *Pseudomonas* thioesterase, this residue is Asp[17] (Fig. 6a). It is positioned within the same monomer as the hydrogen bond donor to the thioester C=O, on the loop connecting the first β-strand to the major α-helix. The

catalytic role of Asp[17] is indeed supported by site-directed mutagenesis experiments, demonstrating that when this residue is replaced with an asparagine, the k_{cat} at 25 °C and pH 7.5 is reduced from 15 s^{-1} to 5 $\times$ 10^{-4} s^{-1} (32). The situation is markedly different in the *Arthrobacter* thioesterase. The residue corresponding to Asp[17] is Gln[58] (Fig. 6b). Inspection of the active site for the *Arthrobacter* thioesterase demonstrates that the only possible candidate for the catalytic base (or nucleophile) is Glu[73], which is on the opposite side of the substrate binding pocket. Site-directed mutation of this glutamate to an alanine residue reduces the k_{cat} at 25 °C and pH 7.5 from 6.7 s^{-1} to 0.0001 s^{-1}.[2] It thus appears that in the *Arthrobacter* protein, the active site base is Glu[73], which is located on the major α-helix of the one monomer of the dimer, whereas the hydrogen bond donor to the thioester C=O is located at the N terminus of the α-helix contributed by the second monomer. The remarkable conclusion drawn from this observation is that

X-ray Structure of a Thioesterase

these two thioesterases (of equivalent catalytic efficiency, substrate specificity, and metabolic function) are apparently employing different regions of the active site scaffold to position the key catalytic carboxylate residue.

Comparison of the Quaternary Structures of the Two Thioesterases—The differences in active site geometries between these two enzymes extends to their quaternary structures as well. Recent ultracentrifugation experiments demonstrate that the *Pseudomonas* thioesterase is also a tetramer. As can be seen in Fig. 2*c*, in the *Pseudomonas* thioesterase, the dimers come together to form the tetramer with their long α-helices facing inwards. The pyrophosphate moieties of the CoA ligands project outwards, and the active site in one dimer is ∼ 21 Å from the symmetry related active site in the second dimer. This arrangement is in sharp contrast to that observed for the *Arthrobacter* enzyme, whereby the dimers combine to form the tetramer with their long α-helices facing outwards (Fig. 2*b*). In the *Arthrobacter* enzyme, the active sites between symmetry-related dimers are ∼27 Å apart, and the pyrophosphate moieties of the CoA ligands project into the dimer-dimer interfacial region. The question arises as to why these two enzymes form tetramers in such remarkably different manners. It appears that the extra N-terminal motif observed in the *Arthrobacter* thioesterase, positioned before the major α-helix, prevents the helix-to-helix face packing as observed in the *Pseudomonas* thioesterase. This additional N-terminal region in the *Arthrobacter* enzyme faces outwards and is not involved in dimer-dimer interactions but is involved in the formation of the active site.

The question of how two bacterial thioesterases, with identical substrates, nearly equal catalytic efficiencies, and similar molecular scaffolds evolved with such different quaternary structures and active site geometries is, indeed, intriguing. Are these thioesterases examples of convergent or divergent evolution? Perhaps the answer lies somewhere between. Regardless of the manner in which these proteins arose, this investigation underscores the importance of a combined kinetic and x-ray crystallographic approach in exploring protein structure/function relationships.

REFERENCES

1. Cork, D. J., and Krueger, J. P. (1991) *Adv. App. Microbiol.* **36,** 1–66
2. Haggblom, M. M. (1992) *FEMS Microbiol. Rev.* **9,** 29–71
3. Higson, F. K. (1992) *Adv. Appl. Microbiol.* **37,** 135–164
4. Furukawa, K. (1994) *Biodegradation* **5,** 289–300
5. Dunaway-Mariano, D., and Babbitt, P. C. (1994) *Biodegradation* **5,** 259–276
6. Yi, H.-R., Min, K.-H., Kim, C.-K., and Ka, J.-O. (2000) *FEMS Microbiol. Ecol.* **31,** 53–60
7. Klages, U., and Lingens, F. (1980) *Hyg. Abt. 1 Orig.* *C* **1,** 215–223
8. Scholten, J. D., Chang, K.-H., Babbitt, P. C., Charest, H., Sylvestre, M., and Dunaway-Mariano, D. (1991) *Science* **253,** 182–185
9. Deleted in proof
10. Deleted in proof
11. Deleted in proof
12. Savard, P., Peloquin, L., and Sylvestre, M. (1986) *J. Bacteriol.* **168,** 81–85
13. Marks, T. S., Wait, R., Smith, A. R., and Quirk, A. V. (1984) *Biochem. Biophys. Res. Commun.* **124,** 669–674
14. Chae, J. C., Kim, Y., Kim, Y. C., Zylstra, G. J., and Kim, C. K. (2000) *Gene (Amst.)* **258,** 109–116
15. Layton, A. C., Sanseverino, J., Wallace, W., Corcoran, C., and Sayler, G. S. (1992) *Appl. Envir. Microbiol.* **58,** 399–402
16. Ruisinger, S., Klages, L., and Lingens, F. (1976) *Arch. Microbiol.* **110,** 253–256
17. Zhuang, Z., Gartemann, K.-H., Eichenlaub, R., and Dunaway-Mariano, D. (2003) *Appl. Envir. Microbiol.* **69,** 2707–2711
18. Benning, M. M., Wesenberg, G., Liu, R., Taylor, K. L., Dunaway-Mariano, D., and Holden, H. M. (1998) *J. Biol. Chem.* **273,** 33572–33579
19. Thoden, J. B., Holden, H. M., Zhuang, Z., and Dunaway-Mariano, D. (2002) *J. Biol. Chem.* **277,** 27468–27476
20. Leesong, M., Henderson, B. S., Gillig, J. R., Schwab, J. M., and Smith J. L. (1996) *Structure* **4,** 253–264
21. Hisano, T., Tsuge, T., Fukui, T., Iwata, T., Miki, K., and Doi, Y. (2003) *J. Biol. Chem.* **278,** 617–624
22. Luo, L., Taylor, K. L., Xiang, H., Wei, Y., Zhang, W., and Dunaway-Mariano, D. (2001) *Biochemistry* **40,** 15684–15692
23. Kabsch, W. (1988a) *J. Appl. Crystallogr.* **21,** 67–71
24. Kabsch, W. (1988b) *J. Appl. Crystallogr.* **21,** 916–924
25. Brunger, A. T., Adams, P. D., Clore, G. M., DeLano, W. L., Gros, P., Grosse-Kunstleve, R. W., Jiang, J. S., Kuszewski, J., Nilges, M., Pannu, N. S., Read, R. J., Rice, L. M., Simonson, T., and Warren, G. L. (1998) *Acta Crystallogr. Sect. D Biol. Crystallogr.* **5,** 905–921
26. Roussel, A., Fontecilla-Camps, J. C., and Cambillau, C. (1990) *Acta Crystallogr. Sect. A* **4,** 66–67
27. Tronrud, D. E., Ten Eyck, L. F., and Matthews, B. W. (1987) *Acta Crystallogr. Sect. A* **43,** 489–501
28. Navaza, J. (1994) *Acta Crystallogr. Sect. A* **50,** 157–163
29. Kraulis, P. J. (1991) *J. Appl. Crystallogr.* **24,** 946–950
30. Lee, B., and Richards, F. M. (1971) *J. Mol. Biol.* **55,** 379–400
31. Li, J., Derewenda, U., Dauter, Z., Smith, S., and Derewenda, Z. S. (2000) *Nat. Struct. Biol.* **7,** 555–559
32. Zhuang, Z., Song, F., Zhang, W., Taylor, K., Archambault, A., Dunaway-Mariano, D., Dong, J., and Carey, P. R. (2002) *Biochemistry* **41,** 11152–11160